Research Article Wiley Online Library ELECTROANALYSIS

DOI: 10.1002/elan.202060597

A Novel Molecule: 1-(2,6 Dichlorobenzyl)-4-(2-(2-4-hydroxybenzylidene)hydrazinyl)pyridinium Chloride and its Interaction with DNA

Ayça Karasakal,[a] Sülünay Parlar,[b] Vildan Alptüzün,[b] Arif E. Cetin,[c] and Seda Nur Topkaya*[d]

Abstract: Herein, a novel pyridine derivative, *1-(2,6 dichlorobenzyl)-4-(2-(2-4-hydroxybenzylidene)-hydrazinyl)pyridinium chloride* (DHPC), was synthesized as a candidate drug molecule. Interaction of DHPC with DNA was used to explore its effect on DNA via Differential Pulse Voltammetry, Cyclic Voltammetry, and Electrochemical Impedance Spectroscopy. We demonstrated that oxidation signal of guanine bases of DNA decreased significantly while that of DHPC increased after its interaction with one another. Our candidate drug molecule exhibits LOD and LOQ, e.g., 1.5 μg/mL and 4.9 μg/mL, respectively. Toxicity effect value for DHPC (S%) was calculated as %31, demonstrating the candidate drug molecule's toxic effect on DNA.

Keywords: DNA · drug molecule · DNA and drug interaction · pyridinium derivative · electrochemical biosensor

1 Introduction

Most drugs target biomolecules such as DNA, RNA or proteins. DNA-drug interaction can be assessed with a wide range of analytical techniques, e.g., UV-Vis Spectroscopy [1], Fluorescence Spectroscopy [2], Mass Spectrometry (MS) [3], Liquid chromatography-mass spectrometry (LC-MS) [4], Nuclear Magnetic Resonance (NMR) [5], Gel Electrophoresis [6], Circular Dichroism Spectroscopy (CDS) [7], Surface Plasmon Resonance (SPR) [8], Molecular Modeling [9], thermodynamic methods [10], and electrochemical methods [11]. Each technique has both advantages and disadvantages. For instance, Florescence Spectroscopy has a high sensitivity and specificity, while its sensitivity is mostly affected with temperature, which limits its application to a broad range of analyte detection. MS requires qualified operators and time-consuming sample preparation steps. LC-MS is an expensive technique due to the need for the isotope-labeled analytes. NMR has low sensitivity as it requires a relatively large amount of samples to for measurement and generates data sets difficult to analyze. SPR is a label-free technique to quantitatively analyze the bindings between molecules in real-time. However, it requires expensive instrumentation and skilled operators. Among these techniques, electrochemical methods are one of the most preferred ones for drug-DNA interaction analyses due to their ability to operate with low quantity of analyte, and simple-to-operate. They can also enable the direct oxidation-based monitoring at low-cost.

In pharmacology, candidate molecules are synthesized to meet the clinical needs, while their use as drugs can be found infeasible after detailed clinical studies. During the discovery of a novel drug, clinical research is conducted if the preclinical steps are successfully accomplished. The candidate molecule after a successful clinical research could be delivered as a medicine in the market [12]. Complexity of the biological systems makes it difficult to simultaneously incorporate these steps into a single algorithm for drug design. Therefore, accurately selecting the candidate molecules is very crucial to use sources effectively, to minimize trial period and to reduce the cost of drug discovery.

In this article, we, for the first time, investigated the electrochemical properties of a novel candidate drug molecule, *1-(2,6 dichlorobenzyl)-4-(2-(4-hydroxybenzylidene hydrazinyl) pyridinium chloride* (DHPC), which is was synthesized as an antimicrobial agent [13]. In literature, there are very few studies with pyridinium salts for the detection of biological molecules, including DNA by taking the advantage of their charged nature [14]. In our previous study, we investigated the electrochemical properties of a novel pyridine derivative, *4-(2-(2-hydroxybenzylidene) hydrazinyl)-1-(3-phenylpropyl) pyridinium bromide (abbreviated as 4-Pyri)*, and its interaction with

[a] A. Karasakal
Department of Chemistry, Faculty of Science and Letters, Namik Kemal University, Tekirdag, Turkey
[b] S. Parlar, V. Alptüzün
Department of Pharmaceutical Chemistry, Faculty of Pharmacy, Ege University,
Izmir, Turkey
[c] A. E. Cetin
Izmir Biomedicine and Genome Center, Izmir, Turkey
[d] S. N. Topkaya
Department of Analytical Chemistry, Faculty of Pharmacy, Izmir Katip Celebi University, 35620, Cigli, Izmir, Turkey
E-mail: sedanur6@gmail.com
sedanur.topkaya@ikcu.edu.tr

Supporting information for this article is available on the WWW under https://doi.org/10.1002/elan.202060597

DNA, where we discovered the fact that 4-Pyri could be used as a potential drug molecule due to its effect on DNA [15]. The structure of pyridinium halides like quaternary nitrogen salts have adsorption properties on negatively charged molecules. For this reason, DHPC molecules could have an effect on negatively charged DNA. Up to now, the effect of DHPC molecules on DNA has not been investigated in literature yet. We first analyzed the electrochemical properties of this novel pyridine derivative. We then explored the interaction between DHPC and DNA molecule via voltammetric techniques as Differential Pulse Voltammetry (DPV), Cyclic Voltammetry (CV), and Electrochemical Impedance Spectroscopy (EIS). We showed that after the interaction between DHPC and DNA, both oxidation currents that belong to DHPC and guanine bases significantly changed. Experimental parameters were investigated in detail, e.g., concentration, type of the supporting electrolyte, and duration of immobilization on the electrode surface.

The developed method for DHPC was tested in terms of linearity, limit of detection (LOD), limit of quantification (LOQ) as well as precision. Furthermore, the value of toxicity effect (S%) was calculated. Our results demonstrated that DHPC strongly interacts with DNA, and it could be used as a potential candidate drug molecule due to its strong impact on DNA.

2 Experimental

2.1 Apparatus

AUTOLAB with NOVA software was used for all electrochemical measurements. Pencil graphite electrodes (PGEs) were used as working electrodes. Ag/AgCl and platinum were used as reference, and counter electrodes, respectively. A Rotring T 0.5 pencil was used as the holder for the graphite lead (Tombo HB model 0.5 mm). Electrical contact with the lead was obtained by soldering a metallic wire to the metallic part.

2.2 Candidate Drug Molecule and DANN

Candidate drug molecule was synthesized according to the method developed by Alptuzun et al. [13]. Chemical structure of DHPC is shown in Figure 1A.

Fish sperm double stranded deoxyribonucleic acid (dsDNA) was supplied from Sigma Aldrich. Stock solutions of DNA and DHPC were prepared by dissolving 1 mg of DHPC in 1 mL of dimethyl sulfoxide, and 1 mg of DNA in 1 mL of purified water, respectively. In our experiments, ultrapure deionized water was used.

Buffer solutions with different contents and pH were used:

ACB: 0.50 M Acetate Buffer (ACB) containing 20 mM NaCl (pH 4.80)

PBS1: 0.05 M Phosphate Buffer (PBS) containing 20 mM NaCl (pH 6.50)

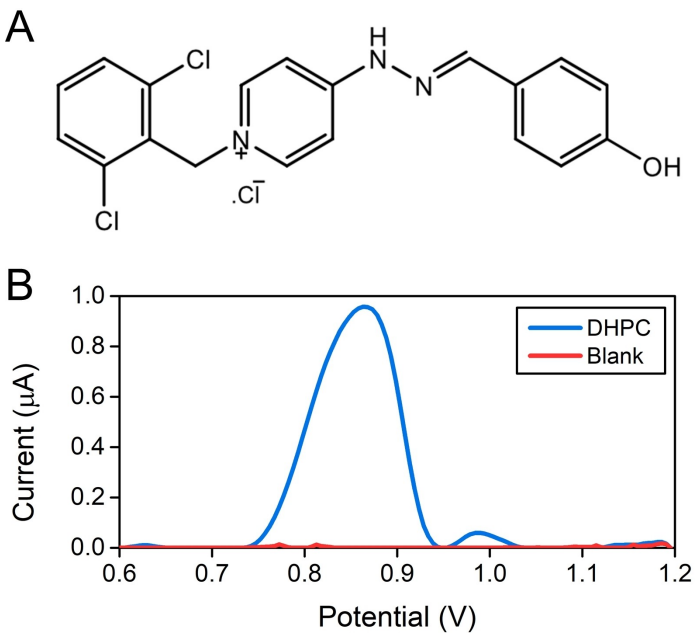

Fig. 1. (A) Chemical structure of DHPC molecule: *1-(2,6 dichlorobenzyl)-4-(2-(4-hydroxybenzylidene hydrazinyl) pyridinium chloride.* (B) DPVs for oxidation currents of DHPC in ACB obtained at +0.85 V and +0.98 V, respectively.

PBS2: 0.05 M Phosphate Buffer (PBS) containing 20 mM NaCl (pH 7.40)

TE: 0.05 M Tris-EDTA (TE) containing 20 mM NaCl (pH 7.80)

BBS: 0.10 M Borate Buffer (BBS) containing 20 mM NaCl (pH 8.10).

2.3 Experimental

PGEs were activated at +1.40 V for 30 sec. in ACB to obtain clean electrode surface. Passive adsorption was selected for both DHPC and DNA for immobilization.

2.3.1 Preparation of DANN

Stock solutions of DNA was diluted with ACB. Activated electrodes were immersed in 200 µg/mL of DNA solution for 1 h and DNA immobilized electrodes were rinsed with ACB.

2.3.2 Preparation of DHPC

Stock solutions of DHPC was diluted with PBS. Activated electrodes were immersed in 100 µg/mL solution for 10 min. Then, DHPC immobilized electrodes were rinsed with PBS.

2.3.3 Interaction of DNA with DHPC

Electrodes first were coated with DNA according to Section 2.3.1. DNA coated electrodes were immersed into a 100 µg/mL DHPC solution prepared in PBS for 90 min. Each DNA-DHPC coated electrodes were rinsed with PBS.

2.3.4 Measurement

We used the oxidation current of DHPC (at +0.85 V vs. Ag/AgCl), and the oxidation current of the guanine bases of DNA (at +1.00 V vs. Ag/AgCl) to evaluate this interaction. In DPV measurements, oxidation current of guanine was measured by scanning from +0.40 V to +1.40 V potential range vs. Ag/AgCl reference electrode with a scan rate of 100 mV/s in ACB. CV measurements were performed between −0.5 and +1.2 V at the scan rate of 50 mV/s in 5 mM $[Fe(CN)_6]^{3-/4-}$ (1:1) prepared in 0.1 M KCl. EIS analyses were measured in the frequency range from 10^5 to 10^{-1} Hz at open circuit potential of +0.25 V vs. Ag/AgCl. Experiments were repeated in triplicate with voltammetric and impedance techniques.

3 Results and Discussion

Until now, we developed different detection strategies to investigate DNA-drug interaction [15–16]. The interaction could exist in different ways, e.g., candidate drug molecules can bind to specific regions in DNA such as a major groove, a minor groove or between DNA bases at specific sequences [17]. In our study, we first examined the redox properties of DHPC, and then explored the underlying mechanisms of the interaction between DHPC and DNA.

3.1 Electrochemical Properties of DHPC

Investigating redox properties of a newly synthesized candidate drug molecule is generally the first step in electrochemical studies. Electrochemical properties of the candidate drug molecule can give kinetic and thermodynamic information about drug absorption, distribution, metabolism, and excretion as well as drug stability. Accordingly, in order to determine the redox properties of DHPC, anodic and cathodic scans were applied with DPV as shown in Figure 1B.

During the potential scan, two anodic peak currents (I_a) were obtained at +0.85 V and +0.98 V. The anodic peak at +0.98 V was quite low as well as not stable compared to the one at +0.85 V (Figure 1B). After changing the direction from positive to negative values, reduction peak currents in the reverse scan were not observed. In addition, DHPC oxidation peak potential obtained from +0.98 V was adjacent to the guanine oxidation window increasing their interference. Therefore, we used the peak potential at +0.85 V as the sensing signal throughout our study.

In general, electrochemical oxidations occur in phenol and hydrazone groups of the compound. Among them, oxidation of phenol forms firstly phenoxy radical, and then it converts to the quinoid radical while oxidation of hydrazone group at 4 position of pyridinium ring result in 1,4-dihydropyridinehydrazone radical.

In order to obtain the most accurate analytical signals, experimental conditions such DHPC concentration, and immobilization time on the electrode surface were optimized as shown in Figure 2. In Figure 2A, oxidation signals of DHPC with concentrations from 20 µg/mL to 200 µg/mL were measured with DPV. For this concentration range, a linear correlation was determined between DHPC concentration and oxidation currents. The highest signal was detected at 100 µg/mL, e.g., this concentration was used in the article. The linear regression equation was determined as $y=0.0052x + 0.552$ ($R^2=0.9993$), where y is the peak current, and x is the DHPC concentration. From this equation, LOD and LOQ were calculated as 1.50 µg/mL and 4.90 µg/mL, respectively. In order to find the optimum immobilization time, 100 µg/mL DHPC was prepared in PBS, and dropped onto the activated electrodes from 5 min to 60 min (Figure 2B). DHPC oxidation current increased after 5 min, and then remained almost constant after 10 min. Therefore, DHPC immobilization time onto the electrode surface was selected as 10 min.

In order to investigate the effect of buffer type, DHPC solution was prepared with ACB (pH 4.80), PBS1 (pH 6.50), PBS2 (pH 7.40), TE (pH 7.80) and BBS (pH 8.10),

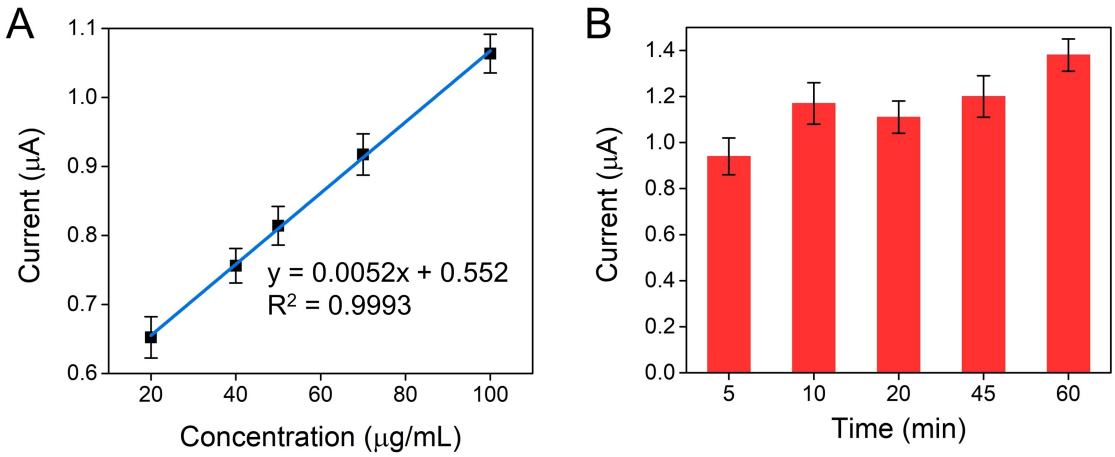

Fig. 2. DHPC optimization study. (A) Calibration plot presenting DHPC oxidation current from 20 to 100 μg/mL DHPC. (B) Histogram for the average DHPC oxidation current for different immobilization time of DHPC on the activated PGE surface from 5 min to 60 min.

and immobilized onto the activated electrodes, where their oxidation signals were measured as shown in Figure 3. Figure 3A shows that DHPC oxidation currents obtained for PBS2, TE and BBS are very close, and they are higher compared to the one obtained for ACB and PBS1. Accordingly, we chose PBS2 for dilution buffer as it provided more stable and well-shaped signals. In order to study the effect of pH on the DHPC peak potential, voltammograms were recorded in the pH range from 4.80 to 8.10. Over this pH range, the anodic peak potential (Ep_a) of DHPC at +0.85 V showed a linearly behavior with pH (Figure 3B), where it shifted to lower potentials with pH. Here, the linear relationship is shown in Equation 1. According to Ep_a – pH data, the equation was found as follows:

$$Ep_a = -0.0859\ pH + 1.2864\ (R^2 = 0.9969) \quad (1)$$

Slope of Equation 1 (86 mV/pH) is different from the ideal slope, e.g., 59 mV/pH, which suggests that the number of transferred protons and electrons are not equal [18].

The effect of scan rate (ν) on DHPC oxidation current (Ipa) was also analyzed with CV. DHPC peak current increased with scan rate in the range between 10 to 100 mV/s (Figure 4).

The relationship between DHPC peak current (Ip_a) and scan rate (ν) shows a linear behavior (Figure 4A):

$$Ip_a(\mu A) = 0.0671\ \nu + 3.5704\ (R^2 = 0.9911) \quad (2)$$

The relationship between DHPC peak current (Ip_a) and the root of the scan rate ($\nu^{1/2}$) also shows a linear behavior (Figure 4B):

$$Ip_a(\mu A) = 0.897\nu^{1/2} + 1.0498\ (R^2 = 0.9907) \quad (3)$$

Such linear behavior was also observed between log(Ip_a) and log(ν) within the scan rate range between 10 mV/s and 100 mV/s (Figure 4C):

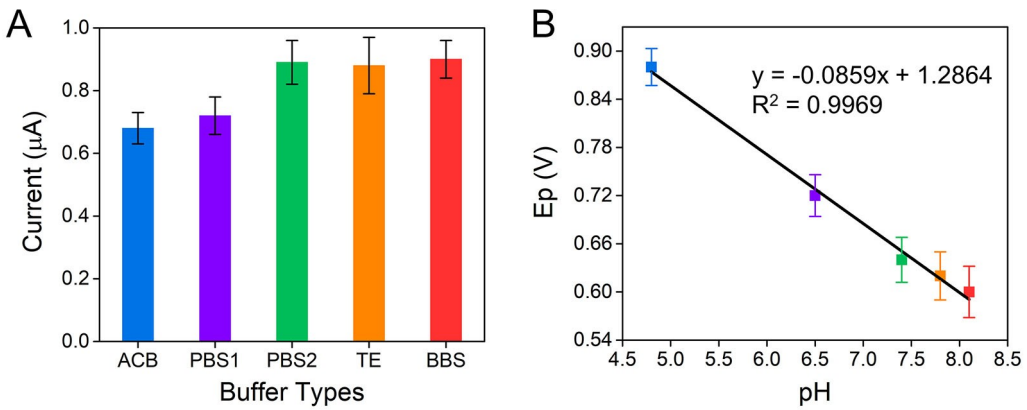

Fig. 3. (A) DPV of DHPC oxidation currents for different buffers. (B) Ep vs. pH, demonstrating the effect of pH on the anodic peak potential (Ep_a) which corresponds to the oxidation of DHPC at +0.85 V.

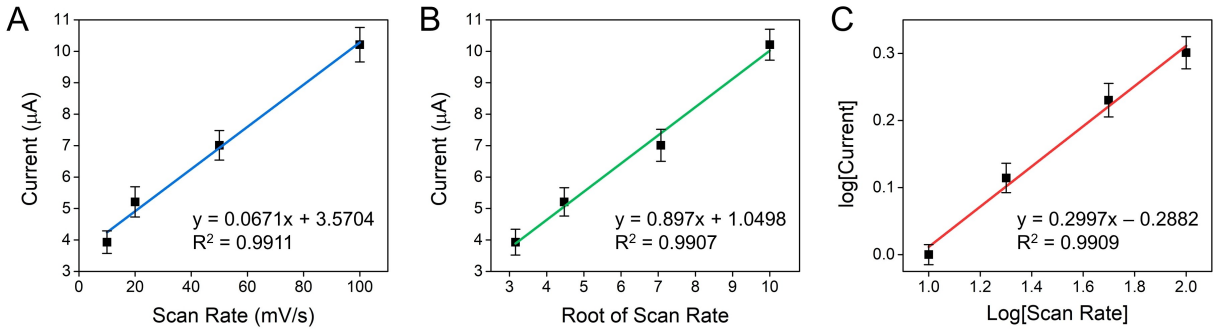

Fig. 4. DHPC peak currents vs. (A) scan rate and (B) roof of the scan rate. (C) Log of the DHPC peak current vs. Log of the scan rate.

$$\log Ip_a = 0.2997\log\nu - 0.2882 (R^2 = 0.9909) \quad (4)$$

The results obtained from Equation 2, 3, and 4 proved that the electrode process was adsorption controlled [19].

3.2 Interaction of DHPC with DNA

Effect of the interaction between DHPC and DNA has been electrochemically investigated by monitoring oxidation signals of DHPC and guanine bases of DNA (Figure 5A). EIS measurements were also performed to further investigate this interaction (Figure 5B). Here, PGEs were modified with DNA, while control experiments were performed where the DNA-modified electrodes were immersed in the supporting electrolyte solution. Electrochemical detection of such interaction was realized via interacting 200 μg/mL DNA with 100 μg/mL DHPC for 90 min (See Supporting Figure S1 for the details of interaction time).

Currents associated with oxidation of the guanine bases in DNA were very high (black curve). However, when DNA coated electrodes were interacted with DHPC, amplitude of the current for guanine oxidation decreased, and shifted to larger positive potentials (red curve). This proves the strong interaction between DHPC and DNA, where the positive potential shift indicates the intercalative interactions between them [18]. As shown in Figure 5A, the oxidation current of DHPC (blue curve) increased significantly after its interaction with DNA. For guanine, the decrease in the oxidation signal was ~31%, while the oxidation signal increased by ~95% for DHPC. In literature, the decrease in guanine oxidation signal due to different interaction pathways was demonstrated [20], while the increase or decrease of intrinsic redox signals of drug molecules are very rare [15, 21]. Therefore, our work is very promising as it evaluates the intrinsic oxidation signals of DHPC, which demonstrates its strong interaction with DNA.

Based on the results for guanine oxidation currents shown in Figure 5A, DHPC's toxicity effect (S%) on DNA was calculated according to Equation 5 [22]:

$$S\% = (S_a/S_b) \times 100 \quad (5)$$

where, S% is the percentage of the guanine peak current change, S_a is the peak current of guanine after the

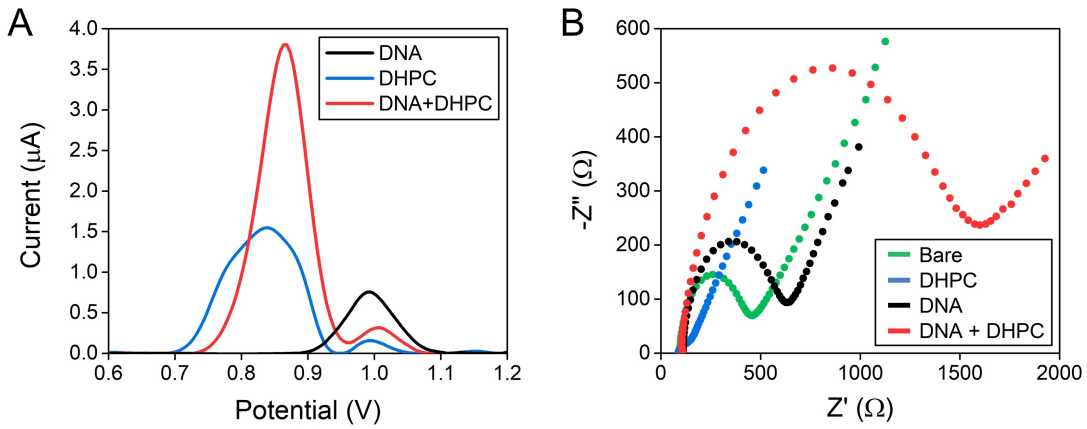

Fig. 5. (A) DPV of oxidation signals for DHPC (+0.85 V) and guanine (+1.00 V) after the interaction between DHPC and DNA under the optimum conditions. (B) The Nyquist diagrams of impedance recorded on bare PGE (green), PGE coated with DHPC (blue), PGE coated with DNA (black), and PGE coated with DNA + DHPC (red) in 0.1 M KCl solution containing 5 mM $[Fe(CN)_6]^{3-/4-}$ (1:1) solution.

interaction with DHPC, and S_b is the peak current of guanine before the interaction with DHPC. Here, if $\%S \geq 85$, drug molecule is non-toxic, and if $\%S \leq 50$, it is toxic to DNA. On the other hand, if the value is between 50 and 85, it is moderately toxic. Using Equation 5, we calculated $S\% = 31$, which shows DHPC's toxicity on DNA.

In addition, we calculated the binding constant for DNA-DHPC interaction using the formula below:

$$dsDNA + DHPC \leftrightarrow dsDNA - DHPC \quad (6)$$

$$\log\frac{1}{[DHPC]} = \log K + \log\frac{I_{dsDNA-DHPC}}{I_{dsDNA} - I_{dsDNA-DHPC}}$$

where K is the binding constant, I_{dsDNA} is the peak current of dsDNA, $I_{dsDNA\text{-}DHPC}$ is the peak current for the dsDNA-DHPC complex. The binding constant K is calculated $2.1 \times 10^3\ M^{-1}$.

Furthermore, EIS was used to characterize the interfacial resistance change during the interaction process. Here, the diameter of the semicircle in Nyquist plot is described by the charge transfer resistance (R_{ct}), and the changes within R_{ct} were evaluated before and after the interaction between DHPC and DNA. As shown in Figure 5B, R_{ct} for bare electrodes (green) increased dramatically after the DNA immobilization (black), which confirms the lower electrical conductivity, and weaker electron transfer ability of redox ions to the electrode surface. R_{ct} values increased more after the interaction between DHPC and DNA (red), which proves the successful immobilization of DHPC on DNA coated electrodes, and their strong interaction. Comparing R_{ct} values of bare electrodes, DHPC coated electrodes (blue) support lower R_{ct}, which proves stronger electron transfer capability.

In our previous study, we investigated the electrochemical properties of a pyridine derivative, 4-(2-(2-hydroxybenzylidene) hydrazinyl)-1-(3-phenylpropyl) pyridinium bromide and its interaction with dsDNA. When we compared the effects of these two molecules on DNA, e.g., 4-Pyri and DHPC, they are both found toxic to DNA. They showed similar voltammetric behaviors. For example, after the interaction of these molecules with DNA, their oxidation currents increased while the guanine signals decreased. For a comparison, the oxidation current of DHPC increased significantly after its interaction with DNA (~95% for DHPC). For 4-Pyri, this rate was 63.55% increase. Guanine signal decrease rate was close to each other, e.g., %52 for 4-Pyri, %31 for DHPC. Furthermore, 4-Pyri gives oxidation signals at +0.6 V and +0.8 V whereas the DPVs for oxidation currents of DHPC in ACB obtained at +0.85 V and +0.98 V because of their structural differences.

4 Conclusion

In this study we, for the first time, investigated the interaction between *1-(2,6 dichlorobenzyl)-4-(2-(2-4-hydroxybenzylidene)hydrazinyl)pyridinium chloride* (DHPC) and DNA. We monitored the changes in the oxidation signal of DHPC and guanine bases of DNA by CV and DPV. We also confirmed the results of the voltammetric studies on the interaction between DHPC and DNA by EIS technique. For DHPC, we showed LOD and LOQ, e.g., 1.5 µg/mL and 4.9 µg/mL, respectively. We determined the toxicity effect of DHPC as %31, which demonstrates its toxic effect on DNA. Our biosensor also exhibited good repeatability and reproducibility.

Acknowledgement

We acknowledge partly financial support from Tekirdag Namik Kemal University (Project No: NKUBAP.00.-.GA.19.217) and Izmir Katip Celebi University (Project No: 2018-GAP-ECZF-0002). Ayca Karasakal acknowledges TUBITAK-BIDEB (1929B011800172) for the support during her stay in Izmir Katip Celebi University.

Data Availability Statement

Data available on request from the authors

References

[1] Q. Zhang, Q. Peng, X. Shu, D. Mo, D. Jiang, *Colloids Surf. B* **2019**, *183*, 110431.
[2] S. Salehzadeh, F. Hajibabaei, N. H. Moghadam, S. Sharifinia, S. Khazalpour, R. Golbedaghi, *J. Fluoresc.* **2018**, *28*, 195–206.
[3] X. Cui, S. Lin, J. Zhou, G. Yuan, *Rapid Commun. Mass Spectrom.* **2012**, *26*, 1803–1809.
[4] H. S. Cho, B. Cho, J. Sim, S. K. Baeck, S. In, E. Kim, *Forensic Sci. Int.* **2019**, *295*, 219–225.
[5] F. Shiri, S. Hadidi, M. Rahimi-Nasrabadi, F. Ahmadi, M. R. Ganjali, H. Ehrlich, *J. Biomol. Struct. Dyn.* **2020**, *38*, 1119–1129.
[6] E. Senkuytu, P. Kizilkaya, Z. Olcer, U. Pala, D. Davarci, Y. Zorlu, H. Erdogan, G. Yenilmez Ciftci, *Inorg. Chem.* **2020**, *59*, 2288–2298.
[7] N. Shakibapour, F. Dehghani Sani, S. Beigoli, H. Sadeghian, J. Chamani, *J. Biomol. Struct. Dyn.* **2019**, *37*, 359–371.
[8] A. Paul, C. Musetti, R. Nanjunda, W. D. Wilson, *Methods Mol. Biol.* **2019**, *2035*, 63–85.
[9] B. J. Denny, R. T. Wheelhouse, M. F. Stevens, L. L. Tsang, J. A. Slack, *Biochemistry* **1994**, *33*, 9045–9051.
[10] S. Afrin, Y. Rahman, T. Sarwar, M. A. Husain, A. Ali, Shamsuzzaman, M. Tabish, *Spectrochim. Acta Part A* **2017**, *186*, 66–75.
[11] a) Z. Yu, X. Chen, Y. Cheng, H. Yang, F. Wang, Z. Chen, *Anal. Chim. Acta* **2021**, *1146*, 140–145; b) S. M. Taghdisi, N. M. Danesh, M. Ramezani, M. Alibolandi, M. A. Nameghi, G. Gerayelou, K. Abnous, *Talanta* **2021**, *223*, 121705; c) H. Akbari Javar, Z. Garkani-Nejad, G. Dehghannoudeh, H. Mahmoudi-Moghaddam, *Anal. Chim. Acta* **2020**, *1133*, 48–57.

[12] J. P. Hughes, S. Rees, S. B. Kalindjian, K. L. Philpott, *Br. J. Pharmacol.* **2011**, *162*, 1239–1249.
[13] V. Alptuzun, S. Parlar, H. Tasli, E. Erciyas, *Molecules* **2009**, *14*, 5203–5215.
[14] a) A. Mazzoli, B. Carlotti, G. Consiglio, C. G. Fortuna, G. Miolo, A. Spalletti, *Photochem. Photobiol. Sci.* **2014**, *13*, 939–950; b) Y. Sun, J. Wang, L. Jin, Y. Chang, J. Duan, Y. Lu, *Polym. J.* **2015**, *47*, 753–759.
[15] S. N. Topkaya, A. Karasakal, A. E. Cetin, S. Parlar, V. Alptüzün, *Electroanalysis* **2020**, *32*, 1780–1787.
[16] a) S. N. Topkaya, A. E. Cetin, *Electroanalysis* **2020**, *32*, 112–118; b) S. N. Topkaya, A. E. Cetin, *Electroanalysis* **2019**, *31*, 1554–1561; c) S. N. Topkaya, V. H. Ozyurt, A. E. Cetin, S. Otles, *Biosens. Bioelectron.* **2018**, *102*, 464–469; d) S. N. Topkaya, G. Serindere, M. Ozder, *Electroanalysis* **2016**, *28*, 1052–1059; e) D. Ozkan-Ariksoysal, O. Akgul, S. Aydinlik, S. N. Topkaya, N. Aladag, M. Ozsoz, *Electroanalysis* **2010**, *22*, 2225–2234.
[17] D. Gibson, *Pharmacogenomics* **2002**, *2*, 275–276.
[18] J. Rupar, M. M. Aleksić, V. Dobričić, J. Brborić, O. Čudina, *Bioelectrochemistry* **2020**, *135*, 107579.
[19] E. Laviron, L. Roullier, *J. Electroanal. Chem. Interfacial Electrochem.* **1980**, *115*, 65–74.
[20] a) K. Lozano Untiveros, E. G. da Silva, F. C. de Abreu, E. F. da Silva-Júnior, J. X. de Araújo-Junior, T. Mendoça de Aquino, S. M. Armas, R. O. de Moura, F. J. B. Mendonça-Junior, V. L. Serafim, K. Chumbimuni-Torres, *Biosens. Bioelectron.* **2019**, *133*, 160–168; b) H. Karimi-Maleh, A. Bananezhad, M. R. Ganjali, P. Norouzi, A. Sadrnia, *Appl. Surf. Sci.* **2018**, *441*, 55–60; c) S. Jahandari, M. A. Taher, H. Karimi-Maleh, A. Khodadadi, E. Faghih-Mirzaei, *J. Electroanal. Chem.* **2019**, *840*, 313–318; d) S. N. Topkaya, V. H. Ozyurt, A. E. Cetin, S. Otles, *Biosens. Bioelectron.* **2018**, *102*, 464–469.
[21] a) B. Öndeş, M. Muti, *Electroanalysis* **2020**, *32*, 1288–1296; b) H. Akbari Javar, Z. Garkani-Nejad, G. Dehghannoudeh, H. Mahmoudi-Moghaddam, *Anal. Chim. Acta* **2020**, *1133*, 48–57.
[22] G. Bagni, D. Osella, E. Sturchio, M. Mascini, *Anal. Chim. Acta* **2006**, *573-574*, 81–89.

Received: April 23, 2021
Accepted: April 30, 2021
Published online on ■■, ■■

RESEARCH ARTICLE

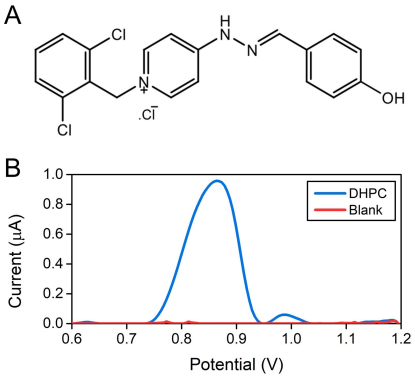

*A. Karasakal, S. Parlar, V. Alptüzün, A. E. Cetin, S. N. Topkaya**